# Tamoxifen Toxicity in Cultured Retinal Pigment Epithelial Cells Is Mediated by Concurrent Regulated Cell Death Mechanisms

Leo A. Kim,[1,2] Dhanesh Amarnani,[1,2] Gopalan Gnanaguru,[1,2] Wen Allen Tseng,[1,2] Demetrios G. Vavvas,[1] and Patricia A. D'Amore[1–3]

[1]Massachusetts Eye and Ear Infirmary, Department of Ophthalmology, Harvard Medical School, Boston, Massachusetts, United States
[2]Schepens Eye Research Institute/Massachusetts Eye and Ear Infirmary, Boston, Massachusetts, United States
[3]Department of Pathology, Harvard Medical School, Boston, Massachusetts, United States

Correspondence: Patricia A. D'Amore, 20 Staniford Street, Boston, MA 02114, USA; patricia_damore@meei.harvard.edu.

Submitted: November 23, 2013
Accepted: June 23, 2014

Citation: Kim LA, Amarnani D, Gnanaguru G, Tseng WA, Vavvas DG, D'Amore PA. Tamoxifen toxicity in cultured retinal pigment epithelial cells is mediated by concurrent regulated cell death mechanisms. *Invest Ophthalmol Vis Sci*. 2014;55:4747–4758. DOI:10.1167/iovs.13-13662

**Purpose.** To evaluate the mechanism of tamoxifen-induced cell death in human cultured RPE cells, and to investigate concurrent cell death mechanisms including pyroptosis, apoptosis, and necroptosis.

**Methods.** Human RPE cells were cultured until confluence and treated with tamoxifen; cell death was measured by detecting LDH release. Tamoxifen-induced cell death was further confirmed by 7-aminoactinomycin D (7-AAD) and annexin V staining. Lysosomal destabilization was assessed using lysosomal-associated membrane protein-1 (LAMP-1) and acridine orange staining. The roles of lysosomal enzymes cathepsin B and L were examined by blocking their activity. Caspase activity was evaluated by caspase-1, -3, -8, and -9 specific inhibition. Cells were primed with IL-1α and treated with tamoxifen; mature IL-1β production was quantified via ELISA. Caspase activity was verified with the fluorochrome-labeled inhibitor of caspases (FLICA) probe specific for each caspase. Regulated cell necrosis or necroptosis was examined with 7-AAD and inhibition of receptor-interacting protein 1 (RIP1) kinase using necrostatin-1 (Nec-1).

**Results.** Cell death occurred within 2 hours of tamoxifen treatment of confluent RPE cells and was accompanied by lysosomal membrane permeabilization. Blockade of cathepsin B and L activity led to a significant decrease in cell death, indicating that lysosomal destabilization and cathepsin release occur prior to regulated cell death. Tamoxifen-induced toxicity was shown to occur through both caspase-dependent and caspase-independent cell death pathways. Treatment of RPE cells with caspase inhibitors and Nec-1 resulted in a near complete rescue from cell death.

**Conclusions.** Tamoxifen-induced cell death occurs through concurrent regulated cell death mechanisms. Simultaneous inhibition of caspase-dependent and caspase-independent cell death pathways is required to protect cells from tamoxifen. Inhibition of upstream activators, such as the cathepsins, may represent a novel approach to block multiple cell death pathways.

Keywords: apoptosis, necroptosis, pyroptosis, RPE, tamoxifen

Tamoxifen, a nonsteroidal estrogen receptor antagonist, has been widely used in low dosages as an adjuvant therapy for some forms of breast cancer. Although the current standard of care is 5 years of tamoxifen therapy, the global Adjuvant Tamoxifen: Longer Against Shorter (ATLAS) trial recently showed that 10 years of tamoxifen treatment reduced the risk of breast cancer recurrence, reduced breast cancer mortality, and reduced overall mortality.[1] Thus, it is likely that the standard of care will change, resulting in a longer period of tamoxifen therapy with a likely increase in tamoxifen-induced ocular toxicity.

Tamoxifen can lead to corneal toxicity, progression of cataracts, retinopathy, and neuropathy. The reported incidence of ocular toxic side effects among patients receiving tamoxifen ranges from 6.3% to 12%. The most visually significant aspect of tamoxifen toxicity is a maculopathy.[2,3] Tamoxifen is structurally similar to other drugs with well-known retinal effects including chloroquine, chlorpromazine, thioridazine, and tilorone. Chloroquine, specifically, has been shown by others to disrupt lysosomal function and disrupt phagocytosis in ARPE-19 cells.[4] Although the RPE is thought to be the primary target of tamoxifen toxicity, recent reports have demonstrated that tamoxifen toxicity also affects photoreceptors.[5] Ultrastructural lesions associated with these agents may appear as crystalloid inclusions in the neuroretina or as crystalloid bodies, within the RPE,[6,7] which are thought to disrupt lysosomal function.

Retinal pigment epithelium cells serve a critical role in the maintenance of photoreceptors, phagocytizing the outer segment tips of photoreceptors, which are then digested within lysosomes. Retinal pigment epithelium dysfunction is thought to play a role in a variety of retinal diseases including AMD, tamoxifen retinopathy, chloroquine retinopathy, central

serous retinopathy, as well as a variety of inherited retinal disorders. Since RPE cells are postmitotic, controlling or preventing cell death in these conditions may help to prevent subsequent photoreceptor degeneration and vision loss.

Cell death commonly occurs through pyroptosis, apoptosis, or necroptosis. Each of these cell death pathways is regulated by distinct molecular mechanisms. For instance, pyroptosis is an inflammatory-mediated form of cell death characterized by activation of caspase-1.[8–11] During pyroptosis, there is an assembly of the inflammasome, a multiprotein complex that activates caspase-1 by facilitating the cleavage of procaspase-1 to active caspase-1. In turn, active caspase-1 mediates the proteolytic maturation of the pro-inflammatory cytokines IL-1β and IL-18 from their inactive precursors to their biologically active forms.[9–13] The NLRP3 inflammasome can be activated by a diverse array of signals.[14] Many of these signals activate NLRP3 by destabilizing lysosomes. For instance, crystalline or insoluble materials such as cholesterol crystals and amyloid-β can activate NLRP3 in phagocytic myeloid-derived cells by disrupting phagolysosomes.[15–18]

In the case of apoptosis, coordinated activation of two groups of caspases: initiators (caspase-2, -8, -9, and -10) and effectors (caspase-3, -6, and -7) are responsible for apoptotic cellular degradation. This type of cell death is characterized by cell shrinkage, nuclear and cytoplasmic condensation, and chromatin fragmentation. Caspases are constitutively present in an inactive precursor form and are cleaved from procaspases to activated caspases; it is the effector caspases that are responsible for cellular degradation. Caspase-3 is the major effector caspase in apoptosis and is activated by several initiator caspases upstream in the signal cascade. Apoptosis can be further divided into various subcategories according to both the stimuli and the pathways leading to execution of cell death. In extrinsic apoptosis, cell death is initiated by caspase-8 after the binding of lethal ligands to their respective death receptor.[8] Once activated, caspase-8 cleaves downstream procaspases by activation of BID (BH3-interacting domain death agonist) and inducing mitochondrial cytochrome *c* release.[19] In intrinsic apoptosis, caspase-9 activation is triggered by intracellular stress, such as DNA damage, oxidative stress, or excitotoxicity,[8] rather than binding of an extrinsic ligand to a death receptor. Activation of caspase-9 leads to mitochondria-mediated activation and cytochrome *c* release into the cytosol.[19,20] Although caspase-8 and caspase-9 represent two distinct apoptotic signaling pathways, both have been shown to activate caspase-3.[21,22]

Necroptosis is characterized by the activation of receptor-interacting protein 1 (RIP1) and RIP3 kinase and is triggered by a variety of stimuli including TNF, DNA damage, and viral infection.[23–26] Cellular components or endogenous adjuvants, such as high-mobility group protein B1, uric acid, galectins, and thioredoxin, released as a consequence of cellular demise, promote an inflammatory response with activation of inflammasomes, cytokine production, inflammatory cell recruitment, and T-cell activation.[27] Necroptosis has been defined as caspase-independent cell death with a necrotic phenotype that can be prevented by the specific RIP1 inhibitor necrostatin-1 (Nec-1).[28,29] Necroptosis has been demonstrated to occur in T lymphocytes, photoreceptors, RPE cells, astrocytes, and neurons and has been suggested to be involved in myocardial infarction.[30–35]

Tamoxifen toxicity of the retina is believed to be mediated by damage to the RPE through disruption of lysosomes.[5] Our laboratory and others have recently demonstrated that RPE cells express components of the NLRP3 inflammasome, which is believed to play a role in AMD through lysosomal destabilization or accumulation of *Alu* RNA resulting from DICER1 deficiency in the RPE.[36,37] We hypothesize that prolonged use of medications such as tamoxifen can disrupt lysosomal membranes, leading to the activation of the NLRP3 inflammasome, release of the pro-inflammatory cytokine IL-1β, and pyroptosis.[38] Here, we report on the involvement of multiple cell death mechanisms in tamoxifen-induced toxicity of the human RPE in culture. Specifically, we examined the roles of inflammasome-mediated pyroptosis, the extrinsic and intrinsic pathways of apoptosis, and RIP kinase–mediated necroptosis.

## Materials and Methods

### Cell Culture of Human ARPE-19 Cells

Human ARPE-19 cells (American Type Culture Collection, Manassas, VA, USA) were cultured in Dulbecco's modified Eagle's medium (DMEM)/F12 medium (Lonza, Walkersville, MD, USA) supplemented with 10% fetal bovine serum (FBS) (Atlanta Biologicals, Lawrenceville, GA, USA), 2 mM L-glutamine (Lonza, Hopkinton, MA, USA), and 100 U/mL penicillin–100 μg/mL streptomycin (Lonza, Hopkinton) in a humidified incubator at 37°C, 10% $CO_2$, and passaged at a ratio of 1:2 to 1:4 using 0.25% trypsin-EDTA (Invitrogen, Carlsbad, CA). The ARPE-19 cells that were grown on cover slips were plated at approximately $6.0 \times 10^4$ cells on 10 μg/mL laminin-coated 12-mm glass cover slips (Sigma-Aldrich Corp., St. Louis, MO, USA) and maintained in the above-mentioned medium until cells were confluent (usually 2 days post plating). The postconfluent cells were maintained in DMEM/F12 medium supplemented with 1% FBS, 2 mM L-glutamine, and 100 U/mL penicillin–100 μg/mL.[39] Cells were used for experiments up to 2 weeks postconfluence.

### Cell Culture of Primary Fetal Human RPE (fhRPE)

Primary fetal human RPE cells (Lonza, Walkersville) were cultured in RPE medium (RtEBM; Lonza, Walkersville) with 5% FBS, 2 mM L-glutamine, and 100 U/mL penicillin–100 μg/mL streptomycin in a humidified incubator for primary cells at 37°C, 5% $CO_2$. These cells were plated at high density on laminin-coated 96-well plates or 0.4-μm polystyrene membrane Transwells coated with laminin (Costar; Corning, Inc., NY, USA) and maintained in RtEBM with 1% FBS medium, 2 mM L-glutamine, and 100 U/mL penicillin–100 μg/mL streptomycin. After 2 weeks of culture, the cells were used for the experiments.

### Tamoxifen Treatment

Tamoxifen (Sigma-Aldrich Corp.) stock solution (108 mM) was prepared in absolute ethanol, according to the manufacturer's recommendation. Cells were treated with different doses of tamoxifen (10, 15, 20, 25, and 30 μM) or 4-OH-tamoxifen (Supplementary Fig. S1). Additionally, ARPE-19 cells were cultured and maintained in 12-well plates and treated with 2, 4, and 8 μM tamoxifen for a period of 2 weeks (Supplementary Fig. S2). The controls received serum free–media containing the same amount of absolute ethanol without tamoxifen. Cytotoxicity of tamoxifen was measured by LDH release.

### Assessment of Cytotoxicity

The conditioned media were collected from ARPE-19 and fhRPE cells of each condition after 120 minutes of treatment, and percentage cell death was quantified by measuring the LDH release in the conditioned media using the CytoTox 96 Non-Radioactive Cytotoxicity Assay (Promega, Madison, WI, USA). As a positive control, the same number of cells maintained in parallel was lysed by two freeze–thaw cycles;

the conditioned media were collected to measure the maximum LDH release. Percentage LDH release was calculated as 100% × (experimental LDH − spontaneous LDH)/(maximal LDH − spontaneous LDH). The early detection of LDH release was observed at 20 to 30 μM; therefore, these concentrations were used to perform all our experiments described below.

### Assessment of Cytoskeletal Changes

Human ARPE-19 cells were seeded on cover slips and treated with or without tamoxifen. The cells were fixed at 15, 30, 45, 60, 90, 120, and 180 minutes using 3% paraformaldehyde, permeabilized using 0.1% Triton X-100, and blocked (3% goat serum, 3% BSA in PBS) for 60 minutes at room temperature (RT). Between each of the steps, the cells were washed with PBS. The cells were then incubated with AlexaFluor 594 phalloidin (1:100) in blocking buffer for 20 minutes, washed, and then the cover slips were mounted using mounting media with Prolong Gold Antifade Reagent with DAPI (Life Technologies, Carlsbad, CA, USA). Images were taken using a Leica AF6000 microscope (Leica, Wetzlar, Germany).

### Immunofluorescence

Human ARPE-19 cells seeded on laminin-coated cover slips and fhRPE cells seeded on Transwells were treated with tamoxifen or control medium, washed, and fixed with 4% paraformaldehyde for 5 minutes. Cells were thoroughly washed in PBS and blocked (10% goat serum or FBS, 0.05% Triton X-100 in PBS) for 60 minutes at RT. Tight junctions and lysosomal integrity were assessed by incubating cells with anti-ZO-1 for the presence of zonula occludens (ZO-1; 1:250 dilution, Life Technologies) or anti–lysosomal-associated membrane protein-1 (LAMP-1; 1:100 dilution, Cell Signaling Technologies, Beverly, MA, USA), respectively. Each primary antibody was prepared in antibody dilution buffer (5% goat serum or FBS and 0.025% Triton X-100 in PBS) and incubated overnight at 4°C. After washing in PBS, cells were incubated with goat anti-rabbit secondary antibody (Life Technologies) at 1:250 dilution for 2 hours at RT. The cover slips were washed and mounted onto slides using Prolong Gold Antifade Reagent with DAPI.

### Quantification of LAMP-1 Immunofluorescence

In order to quantify LAMP-1 immunofluorescence, images of LAMP-1 staining in control and tamoxifen-treated ARPE-19 cells were taken at 0, 30, 90, and 120 minutes using a Leica AF6000 microscope. Within each image, 10 random fields were chosen, and the LAMP-1 fluorescence was measured using ImageJ (Version 1.46; National Institutes of Health, Bethesda, MD, USA). A threshold value was set for red fluorescence intensity using ImageJ; this value was kept constant for quantification of LAMP-1 fluorescence in control and tamoxifen-treated cells. The DAPI-positive nuclei were counted manually.

### Acridine Orange Staining (Supplementary)

Acridine orange staining was performed as previously described[36] to further confirm lysosomal destabilization. Cells were incubated with 5-μM acridine orange (Immunochemistry Technologies, Bloomington, MN, USA) for 30 minutes at 37°C. Cells were washed with PBS followed by treatment with tamoxifen or control medium for 120 minutes. Images of wells were taken over the course of 2 hours on a Nikon Eclipse TE2000 S-microscope (Nikon Instrumentations, Inc., Melville, NY, USA) to evaluate the progression of lysosomal destabilization with time.

### Detection of Necrosis and Apoptosis

Human ARPE-19 cells were seeded onto laminin-coated cover slips at a density of $2.5 \times 10^4$ cells/cover slip (day 0) and grown to confluence. After 2 to 3 weeks in culture, cells were treated with tamoxifen or control medium. Cells were washed with serum-free medium at 30, 60, 90, and 120 minutes and then incubated with fluorescent-conjugated 7-aminoactinomycin D (7-AAD), a dye for cell viability and early necrosis, (1:100; Enzo Life Sciences, Farmingdale, NY, USA) or the apoptosis marker annexin V (1:50; Life Technologies) for a period of 30 minutes at 37°C. The cells were washed and fixed with 2% paraformaldehyde for 5 minutes followed by washes with PBS. The cover slips were mounted onto slides using Prolong Gold Antifade Reagent with DAPI. Images were taken using a Leica AF6000 microscope for analysis and identification of 7-AAD and annexin V–positive cells.

### Detection of Caspase Activation

Activation of various caspases was measured using the fluorochrome-labeled inhibitor of caspases (FLICA) probes for caspase-1 (FAM-YVAD-FMK), caspase-3 (FAM-DEVD-FMK), caspase-8 (FAM-IETD-FMK), and caspase-9 (FAM-LEHD-FMK) (Immunohistochemistry Technologies), as previously described.[36] The cells were protected from light and pretreated with FLICA for 2 hours prior to incubation with tamoxifen or control media at 37°C, 10% $CO_2$. Following incubation with tamoxifen or control media for 60, 90, and 120 minutes, samples were washed, and the cell nuclei were stained with Hoechst 33342 (Immunohistochemistry Technologies). The samples were washed and fixed, using wash buffer and fixative supplied with the FLICA Kit, and imaged using a Leica AF6000 microscope.

### Inhibition of RIP1 Kinase, Caspases, and Cathepsins

Human ARPE-19 cells maintained in 12-well plates were treated with tamoxifen alone or in combination with inhibitors as follows: RIP1 kinase inhibitor, necrostatin-1 (30 μM; Sigma-Aldrich Corp.); pan-caspase inhibitor, Z-VAD-FMK, caspase-1 inhibitor Z-YVAD-FMK, caspase-3 inhibitor Z-DEVD-FMK, caspase-8 inhibitor Z-IETD-FMK, caspase-9 inhibitor Z-LEHD-FMK (10 μM; all from BioVision, Mountain View, CA, USA); cathepsin B/L inhibitor Z-FF-FMK, specific cathepsin B inhibitor CA-074-Me, and/or cathepsin L inhibitor Z-FY(t-Bu)-FMK (20 μM; all from EMD Millipore, Billerica, MA, USA). After 120 minutes of treatment, cells were washed and imaged using the Nikon Eclipse TE2000 S-microscope.

### Quantification of IL-1β Secretion

Human ARPE-19 cells were seeded onto 12-well plates in complete media and grown to confluence. The cells were primed for 48 hours with 10 ng/mL IL-1α as described previously.[36] After 48 hours, the cells were treated with treated with 10, 20, and 30 μM tamoxifen. Dimethyl sulfoxide (DMSO) vehicle was used as negative control; and 1 mM L-leucyl-L-leucine methyl ester (Leu-Leu-OMe; Chem-Impex International, Wood Dale, IL, USA) was used as positive control, as it had been shown previously to induce release of mature IL-1β.[15,36] Conditioned media were collected after 3 hours, and IL-1β was quantified via ELISA (BD Biosciences, Franklin, NJ, USA). Values were corrected for release of pro-IL-1β because of cytotoxicity using the method described by Miao and colleagues.[40]

Investigative Ophthalmology & Visual Science

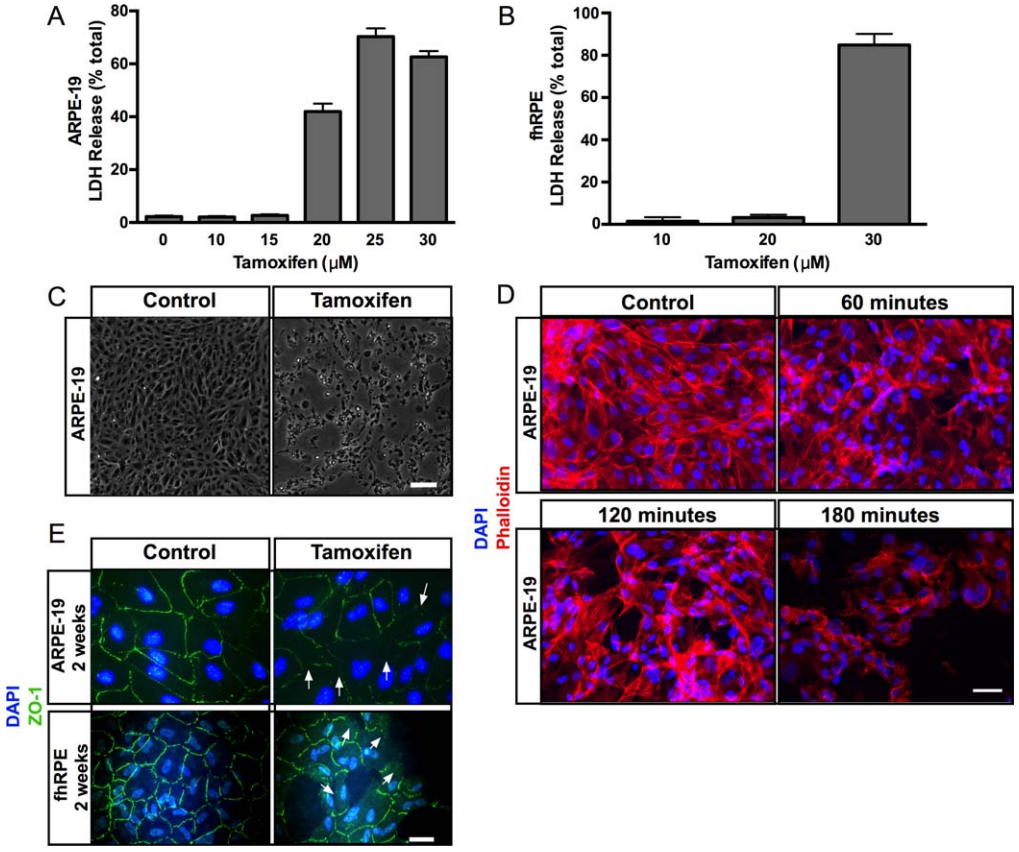


**Figure 1.** Tamoxifen induces cytotoxicity in ARPE-19 and fhRPE cells. Increasing doses of tamoxifen treatment led to an increase in LDH release in (**A**) ARPE-19 cells, and (**B**) in fhRPE cells. (**C**) Light micrographs of control and tamoxifen-treated ARPE-19 cells. Cells exposed to tamoxifen (*right*) appear round and show patches of cell loss when compared with controls (*left*). *Scale bar*: 200 μm. (**D**) Phalloidin staining (*red*) of control cells (*top left*) shows normal actin cytoskeletal organization, and DAPI staining reveals the nuclei *(blue*). Progressive loss of actin cytoskeletal organization was observed with 60, 120, and 180 minutes of tamoxifen treatment (*top right and bottom*). *Scale bar*: 25 μm. (**E**) Immunofluorescence micrographs demonstrated normal hexagonal arrangement of the tight junction protein ZO-1 (*green*) in control ARPE-19 and fhRPE cells (*left, top and bottom*); tamoxifen-treated ARPE-19 and fhRPE cells show disruption and loss of ZO-1 staining (*arrows at right top and bottom*). *Scale bar*: 25 μm. *Error bars*: ±SEM.

### Western Blots (Supplementary)

Human ARPE-19 cells were lysed using 1× radio-immunoprecipitation assay (RIPA) buffer (Cell Signaling Technologies) containing Complete Mini EDTA-free Protease Inhibitor Tablet (Roche, Indianapolis, IN, USA), 2 mM phenyl methanesulfonyl fluoride (PMSF), and 2 mM sodium orthovanadate (NaOV), and then sonicated on ice. Protein concentrations were measured, and equal concentrations of protein were separated using 10% polyacrylamide gels and transferred to polyvinylidene difluoride (PVDF) membranes (Millipore, Billerica, MA, USA). Membranes were blocked for 1 hour at RT in 3% BSA in Tris-buffered saline with 0.1% Tween 20 (TBS-T), followed by incubation with anti-RIP3 antibody (1:1000 in 1% BSA; Abcam, Cambridge, MA, USA) overnight at 4°C. After washes in TBS-T, membranes were incubated for 1 hour at RT in horseradish peroxidase (HRP)-linked secondary antibodies anti-mouse and anti-rabbit IgG (1:10,000 in blocking buffer; GE Healthcare, Pittsburgh, PA, USA). Following additional washes in TBS-T, proteins were visualized by enhanced chemiluminescence using SuperSignal substrates (Thermo Scientific, Tewksbury, MA, USA). Membranes were stripped and then reprobed with rabbit anti-RIP1 (1 μg per 1 mg of protein; BD Biosciences) overnight at 4°C, washed with TBS-T, and incubated for 1 hour at RT with HRP-linked secondary antibodies prior to visualization with enhanced chemiluminescence.

### Data Analysis and Statistics

Data are presented as mean ± SEM of at least three independent experiments unless otherwise indicated. Statistical significance was evaluated using a one-way ANOVA followed by post hoc Tukey-Kramer multiple comparison tests, using the Prism 6.0 software package (GraphPad Software, Inc., La Jolla, CA, USA). Adjusted $P$ values $< 0.05$ were considered statistically significant.

## Results

### Tamoxifen Induces Cell Death in Cultured ARPE-19 and fhRPE Cells

Several studies indicate that tamoxifen induces cytotoxicity that specifically affects RPE and photoreceptor cells.[5,41] In order to investigate the mechanism of tamoxifen-induced RPE cell death, we treated ARPE-19 cells and primary fhRPE cells with different doses of tamoxifen. This study revealed that tamoxifen induced RPE cytotoxicity in a dose-dependent manner (Figs. 1A, 1B). Two-hour exposure of confluent ARPE-19 cells to 10 and 15 μM tamoxifen had little effect on cell viability, whereas exposure to 20, 25, and 30 μM tamoxifen induced 40% to 70% LDH release. Two-hour exposure of confluent fhRPE cells to 10 and 20 μM tamoxifen had little effect on cell viability, whereas exposure to 30 μM tamoxifen

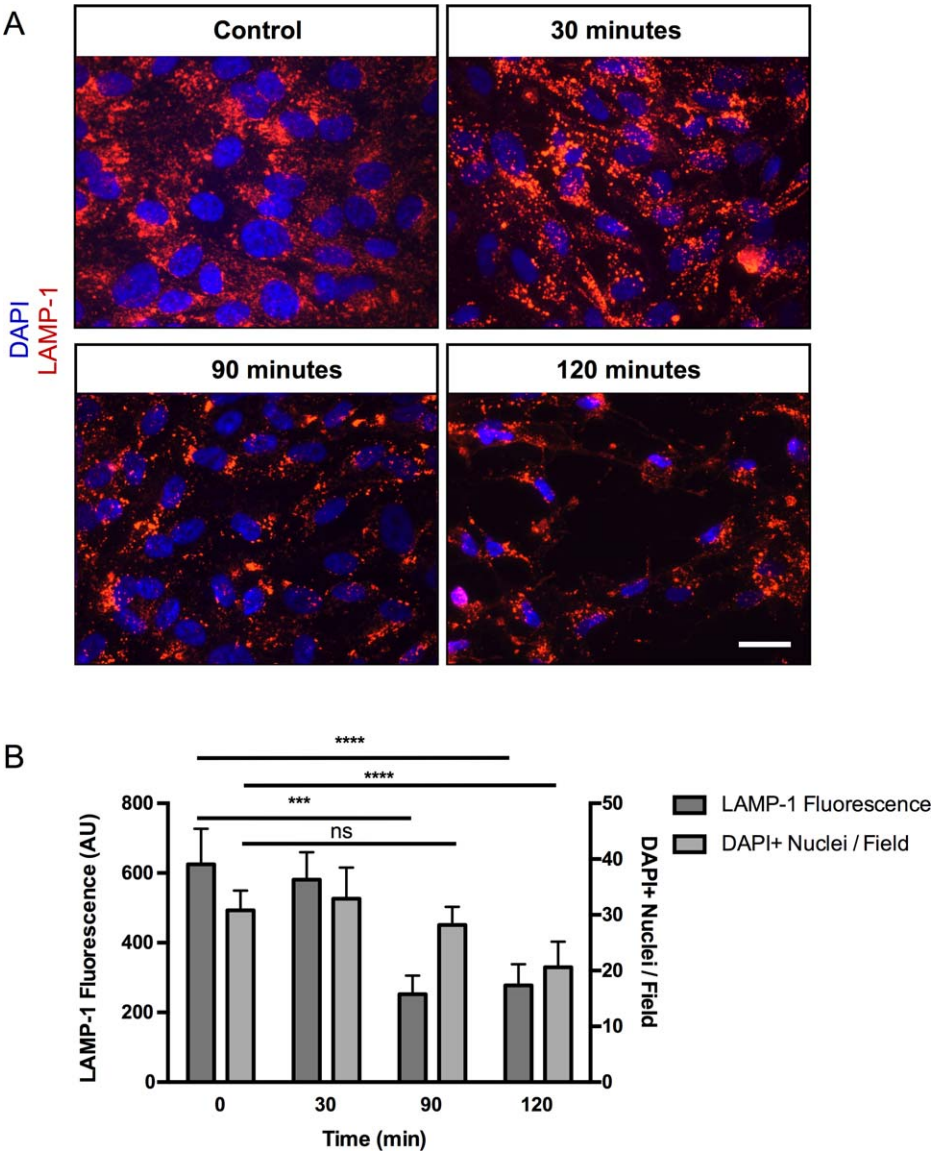


**Figure 2.** Tamoxifen toxicity causes lysosomal destabilization. (**A**) LAMP-1 (*red*) was localized to lysosomes in ARPE-19 cells by immunofluorescence in control cells (*top left*), and a progressive loss of LAMP-1 staining was observed with 30, 90 and 120 minutes of tamoxifen treatment (*top right and bottom*). *Scale bar*: 25 μm. (**B**) Quantification of LAMP-1 staining showed a statistically significant decrease in LAMP-1 fluorescence after 90 minutes, with no significant difference in cell counts when compared with the control. After 120 minutes, there was a statistically significant decrease in both LAMP-1 fluorescence and cell count as determined by DAPI+ nuclei. *Error bars*: ±SEM. Adjusted *P* values: $^{***}P < 0.005$, $^{****}P < 0.0001$.

resulted in 85% LDH release (Fig. 1B). Exposure to 4-OH-tamoxifen, one of the primary active metabolites of tamoxifen metabolized by CYP2D6, induced LDH release in a dose-dependent fashion (Supplementary Fig. S1). Two-hour exposure of cells to 10 to 20 μM 4-OH-tamoxifen had limited LDH release, whereas exposure of confluent ARPE-19 cells to 30 to 60 μM 4-OH-tamoxifen induced 48% to 98% LDH release. Long-term exposure (over 2 weeks) of 2, 4, and 8 μM tamoxifen induced 19%, 19%, and 79% of LDH release, respectively (Supplementary Fig. S2).

In addition, tamoxifen-treated cells exhibited features of cell death including swollen cell bodies, shrinkage, blebbing, and detachment from the culture substrate (Fig. 1C). Visualization of actin cytoskeleton and ZO-1 distribution further validated these observations (Figs. 1D, 1E). Phalloidin staining displayed intact cytoskeletal organization in controls, whereas tamoxifen treatment resulted in a loss of actin stress fibers by 60 minutes of treatment (Fig. 1D). Similarly, differentiated 2-week-old ARPE-19 and fhRPE cells exposed to tamoxifen and stained with antibodies to ZO-1 revealed loss of ZO-1 staining upon exposure to tamoxifen (Fig. 1E).

## Tamoxifen Induces Loss of Lysosomal Integrity in ARPE-19 Cells

Our lab, as well as others, has demonstrated that disruption of lysosomal integrity induces RPE cell death through pyroptosis.[36] To test if tamoxifen treatment induces RPE cell death through lysosomal destabilization, lysosomal integrity was assessed by analyzing LAMP-1 immunofluorescence staining in differentiated ARPE-19 cells. Time-course studies showed a statistically significant reduction of LAMP-1 staining at 90 minutes when compared with the initial control time point (252 vs. 625 AU, respectively), with no significant decrease in

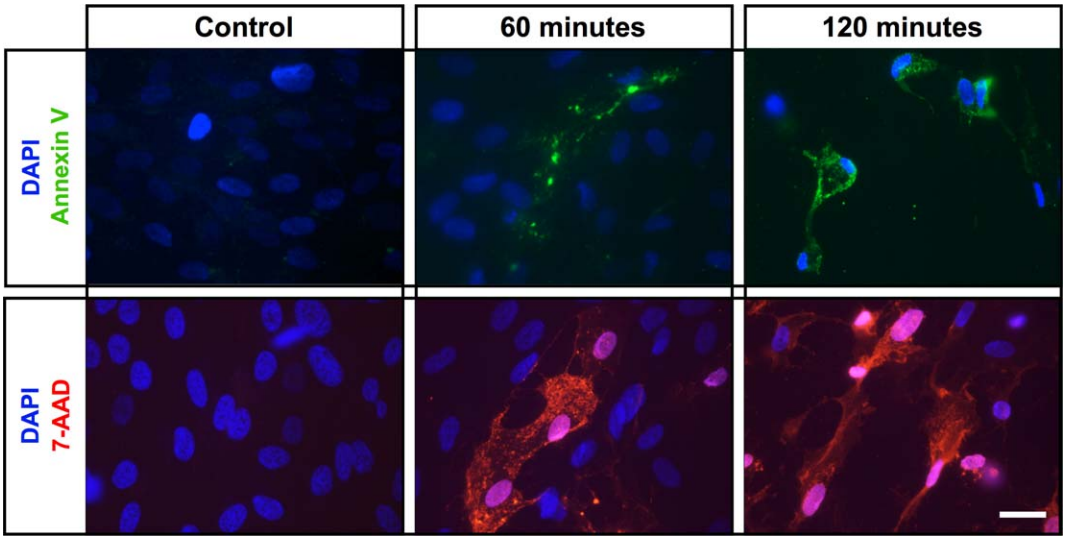


FIGURE 3. Necrotic and apoptotic cell death pathways are activated by tamoxifen toxicity. Staining of control (no tamoxifen) ARPE-19 cells (*left top and bottom*) with annexin V (*green*) or 7-AAD (*red*) shows no apoptotic or necrotic positive cells, respectively. Staining of tamoxifen-treated ARPE-19 cells with annexin V (*green, upper*) or 7-AAD *(red, bottom*) shows both apoptotic and necrotic cells; DAPI (*blue*) shows nuclear staining. *Scale bar*: 25 μm.

cell counts (28 vs. 31, DAPI+ nuclei, respectively) (Fig. 2). However, at 120 minutes, when compared with the initial control time point, there was a statistically significant reduction of both LAMP-1 fluorescence and cell count (277 vs. 625 AU and 21 vs. 31 DAPI+ nuclei, respectively). Lysosomal integrity was further assessed by acridine orange staining, which labels nucleic acids in green and lysosomes in red. Untreated ARPE-19 cells displayed punctate red-orange structures, characteristic of intact lysosomes, whereas treatment with tamoxifen resulted in loss of lysosomal staining after 20 minutes (Supplementary Fig. S3). Taken together, these data indicate that lysosomal destabilization occurs prior to cell death.

## Apoptotic and Necrotic Cell Death Occur Following Tamoxifen Treatment

The data thus far indicate that tamoxifen treatment leads to RPE cytoskeletal disruption resulting in cell death (Figs. 1, 2), but it is unclear whether tamoxifen triggers a specific cell death pathway. To investigate the mechanism of cell death, we used annexin V, which recognizes phosphatidylserine exposed on the cell surface during apoptosis, on ARPE-19 cells cultured for 2 weeks on laminin-coated coverslips.[42] Staining with annexin V revealed apoptotic cell death with increasing fluorescence upon application of tamoxifen when compared with the control (Fig. 3, top row). Of interest, we found that at 60 minutes, only a subset of cells stained with annexin V. To test if tamoxifen induces other possible mechanisms of cell death, we analyzed for 7-AAD,[43] an early necrosis marker that selectively binds to GC regions of DNA.[44] There was a time-dependent increase in 7-AAD staining upon exposure to tamoxifen and no 7-AAD staining in the controls (Fig. 3, bottom row). As with annexin V staining, at 60 minutes, only a subset of cells stained positive for 7-AAD. Together, these data suggest that tamoxifen induces RPE cell death through multiple cell death pathways, as both necrosis and apoptosis appear to be activated following tamoxifen treatment.

## Tamoxifen Activates Caspases That Mediate Pyroptosis and Apoptosis in ARPE-19 Cells

We showed that tamoxifen treatment destabilizes lysosomes (Fig. 2). Destabilization of lysosomes has been shown to induce the NLRP3 inflammasome through the activation of caspase-1,[36] which has been shown to mediate pyroptosis.[45] We therefore used a fluorescence-based FLICA assay to investigate if tamoxifen treatment activates caspase-1 or any other caspases that mediate cell death. Caspase-1 was activated within 60 minutes of tamoxifen exposure, with increasing levels of staining at 90 and 120 minutes (Fig. 4, row 1). No caspase-1 activation was observed in the controls (Fig. 4, row 1). We then evaluated the activation of apoptosis initiators caspase-8 and caspase-9, with and without tamoxifen treatment. The control cells showed no activation of either caspase-8 or caspase-9 during the experimental time period (Fig. 4, rows 2 and 3), whereas both caspase-8 and caspase-9 activation was observed after 60, 90, and 120 minutes of tamoxifen treatment (Fig. 4, rows 2 and 3). Activation of caspase-8 and caspase-9 leads to the activation of the effector caspase-3, which we observed to be minimally activated at 60 minutes, but more pronounced staining was observed at 90 and 120 minutes (Fig. 4, row 4). These results demonstrate that tamoxifen toxicity activates caspase-mediated cell death pathways including pyroptosis and apoptosis.

## Combinatorial Inhibition of Necroptosis, Pyroptosis, and Apoptosis Prevents Tamoxifen-Induced Cell Death

Our results indicate that RPE cell death is mediated through caspase-dependent and caspase-independent mechanisms. To test the relative contribution of the various mechanisms to tamoxifen-induced RPE cell death, we treated ARPE-19 cells with inhibitors specifically targeted against pyroptosis, apoptosis, and necroptosis in the presence of 20 μM tamoxifen.

ARPE-19 cells express the mediators of necroptosis, RIP1, and RIP3 kinases (Supplementary Fig. S4), and treatment of tamoxifen activates the early necrosis marker 7-AAD (Fig. 3). Therefore, we tested the effect of Nec-1, a selective inhibitor of RIP1 kinase, on tamoxifen-induced ARPE-19 cell death. The treatment of Nec-1 in the presence of tamoxifen reduced LDH release by 80% when compared with the tamoxifen only–treated control, which showed 73% LDH release (Fig. 5A).

We next analyzed the role of the various caspases in tamoxifen-induced ARPE-19 cell death. Of interest, treatment

Investigative Ophthalmology & Visual Science

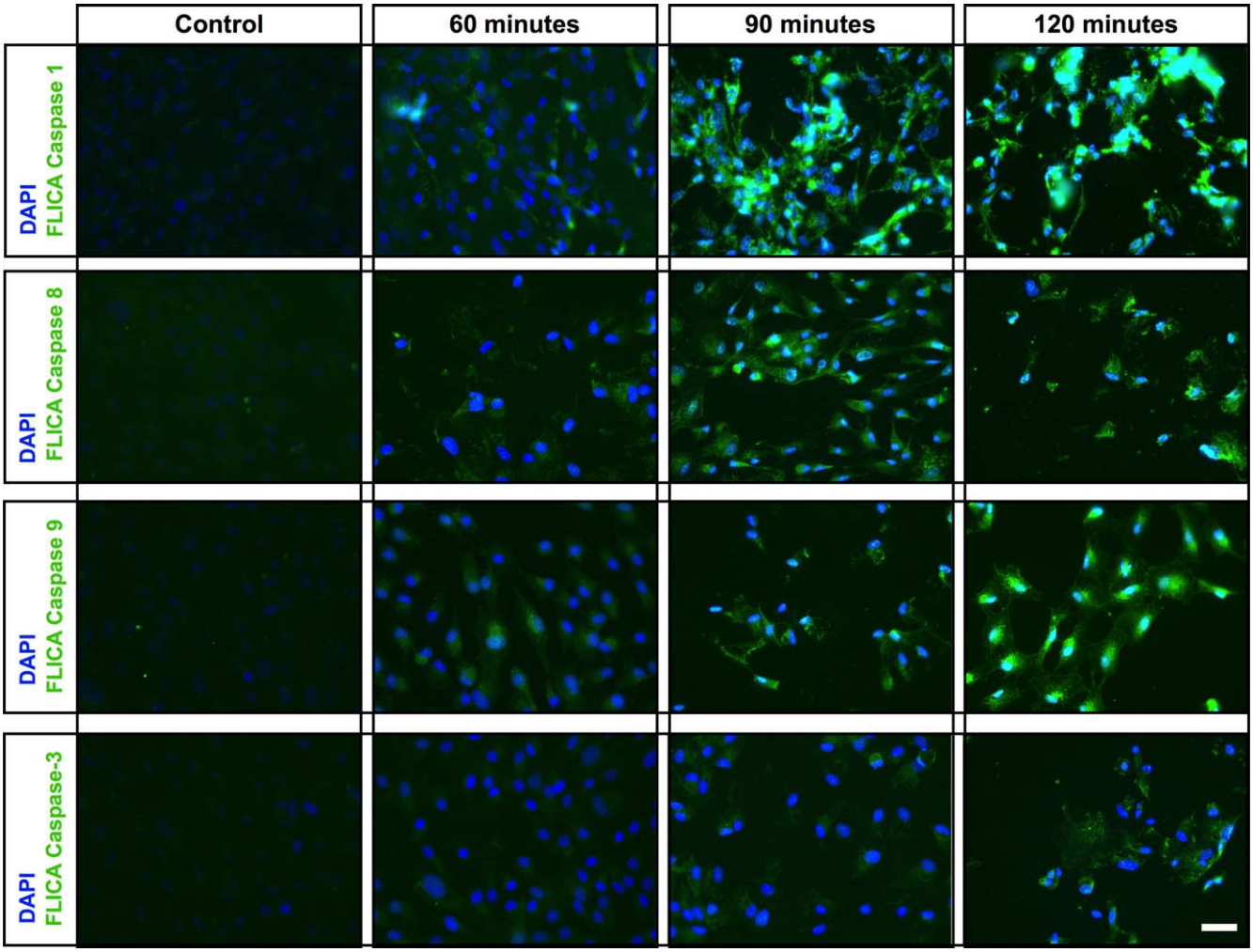


Figure 4. Treatment of ARPE-19 cells with tamoxifen results in caspase activation. Active caspase-1, -8, -9, and -3 levels were detected using the FAM-FLICA Assay Kit (*green*). Control cells show almost no caspase (-1, -8, -9, and -3) activity (*left*). Active caspase-1 was detected as early as 60 minutes of exposure to tamoxifen, and the levels increased at 90 and 120 minutes (*row 1*). Activation of the initiator caspases, caspase-8 and caspase-9 (activators of caspase-3) was observed after 60 minutes of tamoxifen treatment, with increasing levels of fluorescence observed at 90 and 120 minutes (*rows 2* and *3*). Activation of caspase-3 (*green*), the effector caspase, was observed 90 minutes after application of tamoxifen, 30 minutes later than the activation of caspase-8 and caspase-9. Continued caspase-3 activation occurred over time, as increased fluorescence was observed 120 minutes following tamoxifen treatment. *Scale bar*: 25 μm.

with a pan-caspase inhibitor did not prevent tamoxifen toxicity (Fig. 5A); this could be due to a nonspecific or off-target effect, such as activation of alternate cell death pathways. In contrast, treatment of ARPE-19 cells with the caspase-1–specific inhibitor (Z-YVAD-FMK) and the caspase-3 inhibitor (Z-DEVD-FMK) partially rescued ARPE-19 cells from tamoxifen toxicity (Fig. 5A). Treatment of ARPE-19 with caspase-1 and -3 inhibitors led to a reduction in LDH release, with 50% and 40% LDH release, respectively. Concurrent treatment of Nec-1 with either pan-caspase, caspase-1, or caspase-3 inhibitors resulted in more effective inhibition of cell death when compared with the individual caspase inhibitors alone after 2 hours of treatment with tamoxifen (Figs. 5A, 5B; Supplementary Fig. S5). We also investigated whether the initiators of apoptosis, caspase-8 or -9 play a role in tamoxifen-induced RPE cell death. Inhibition of caspase-8 did not decrease LDH release, while caspase-9 inhibition significantly decreased LDH release when compared with tamoxifen control (Fig. 5C). Treatment with a combination of Nec-1 and either caspase-8 or caspase-9 inhibitor more effectively blocked tamoxifen-induced LDH release than use of any of the inhibitors alone (Fig. 5C).

We speculate that the release of lysosomal cathepsins is the upstream activator of cell death pathways. This is supported by the observation that the dual cathepsin B/L inhibitor (Z-FF-FMK) significantly reduced tamoxifen toxicity, reducing LDH release by 90% (Fig. 5A). Next, we tested whether inhibition of cathepsin B or L alone could block tamoxifen toxicity. Treatment of tamoxifen-treated ARPE-19 cells with a cathepsin L (Z-FY[t-Bu]-DMK) or cathepsin B (CA-074-Me) inhibitor each significantly reduced LDH release (Fig. 5D), but inhibition of both cathepsin B and L almost completely blocked LDH release (Fig. 5D).[46]

## Caspase-1 Activation Leads to Production of IL-1β

The activation of caspase-1 can induce pyroptosis as well as lead to the release of the pro-inflammatory cytokine, mature IL-1β. To investigate if the activation of caspase-1 resulting from tamoxifen toxicity also leads to mature IL-1β release, ARPE-19 cells were primed with IL-1α for 24 hours to induce expression of IL-1β precursor, pro-IL-1β. We were unable detect mature IL-1β release in unprimed ARPE-19 cells treated with tamoxifen

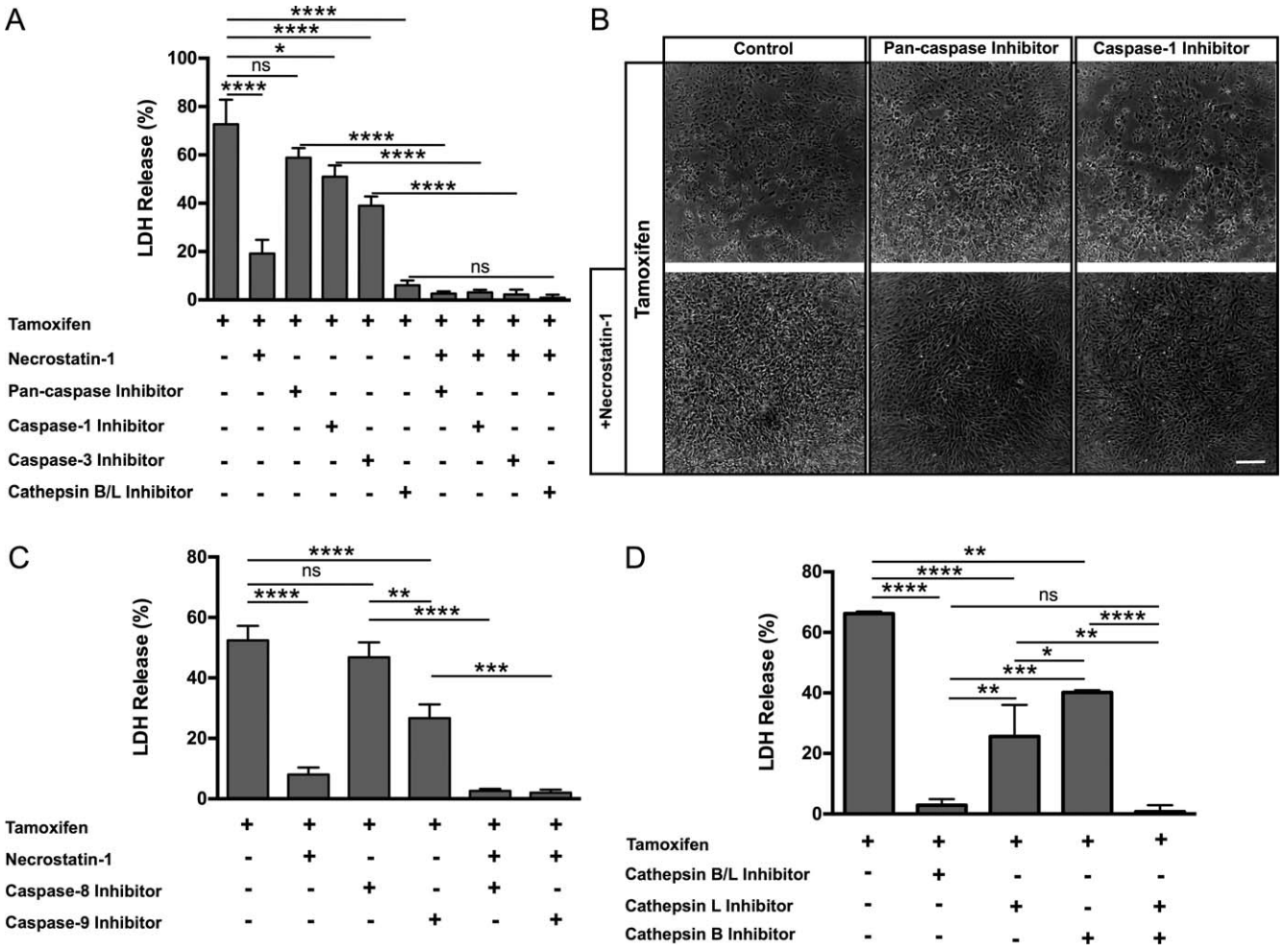


**Figure 5.** Inhibition of cell death pathways decreases tamoxifen-mediated ARPE-19 cytotoxicity. (**A**) Treatment of tamoxifen-exposed ARPE-19 cells with inhibitors for Nec-1, caspase-1, caspase-3, or cathepsin B/L significantly reduced cell death (as measured by LDH release). Combining caspase or cathepsin inhibitors with Nec-1 further significantly reduced tamoxifen-mediated cell death, as compared to treatment with caspase and cathepsin inhibitors alone. (**B**) Abnormal morphology of ARPE-19 cells was observed after tamoxifen administration, with rounded cells and patches of cell loss visible (*top left*). Treatment of ARPE-19 cells with Nec-1 (*bottom row, first section*) and pan-caspase inhibitors (*top row, second section*) alone inhibited cell death, but cellular morphology appeared abnormal, suggesting cell distress. Caspase-1 inhibitor treatment alone partially rescued cell death; however, abnormal cellular morphology was still observed (*top row, third section*). Combinatorial treatment of Nec-1 with pan-caspase inhibitor (*bottom row, second panel*) or Nec-1 with caspase-1 inhibitor (*bottom row, third section*) resulted in near complete inhibition of cell death and preservation of normal morphology (as shown in Fig. 1C). *Scale bar*: 200 μm. (**C**) The LDH assay reveals that inhibition using a combined cathepsin B/L inhibitor significantly reduced LDH release. Inhibition of cathepsin B or cathepsin L alone shows moderate reduction of LDH release in tamoxifen-induced ARPE-19 cytotoxicity when compared with the controls. Concurrent inhibition with individual cathepsin B and cathepsin L inhibitors drastically reduced LDH release with tamoxifen treatment, similar to use of the combined cathepsin B/L inhibitor. (**D**) Inhibition of caspase-9, but not caspase-8, significantly reduced LDH release in tamoxifen-treated ARPE-19 cells. Inhibition of caspase-8 together with Nec-1 or inhibition of caspase-9 along with Nec-1 dramatically reduced LDH release. *Error bars*: ±SEM. Adjusted *P* values: $^{**}P < 0.05$, $^{***}P < 0.005$, $^{****}P < 0.0001$.

(data not shown). Treatment of primed ARPE-19 cells with different concentrations of tamoxifen resulted in the release of mature IL-1β in a dose-dependent manner (Fig. 6A). Maximal production of mature IL-1β (8.6 pg/mL) was observed with 30 μM tamoxifen treatment (Fig. 6A). Nec-1 treatment did not significantly alter IL-1β production, but inhibition of caspase-1 resulted in a 64% decrease in mature IL-1β secretion from 17.6 pg/mL to 6.4 pg/mL (Fig. 6B).[36]

## Discussion

It has been shown that tamoxifen toxicity can lead to visual defects[2,3] and is likely associated with damage to RPE and photoreceptors.[5] The goal of this study was to investigate the mechanism by which tamoxifen induces RPE cell death and identify targets that can be used as a potential therapy. We examined the mechanism of tamoxifen toxicity in cultured RPE cells and demonstrated that tamoxifen-induced lysosomal destabilization is associated with the activation of a number of cell death pathways. Initial lysosomal destabilization in ARPE-19 cells was followed by release of cathepsins, which were observed to play a major role in initiating multiple cell death mechanisms: pyroptosis, apoptosis, and necroptosis. Dual inhibition of cathepsins B and L completely prevented tamoxifen-induced RPE cell death.

Cell death can occur through several different mechanisms. One event that may initiate cell death is lysosomal destabilization. Permeabilization of lysosomal membranes leads to the release of hydrolases such as the cathepsins, which have been

Investigative Ophthalmology & Visual Science

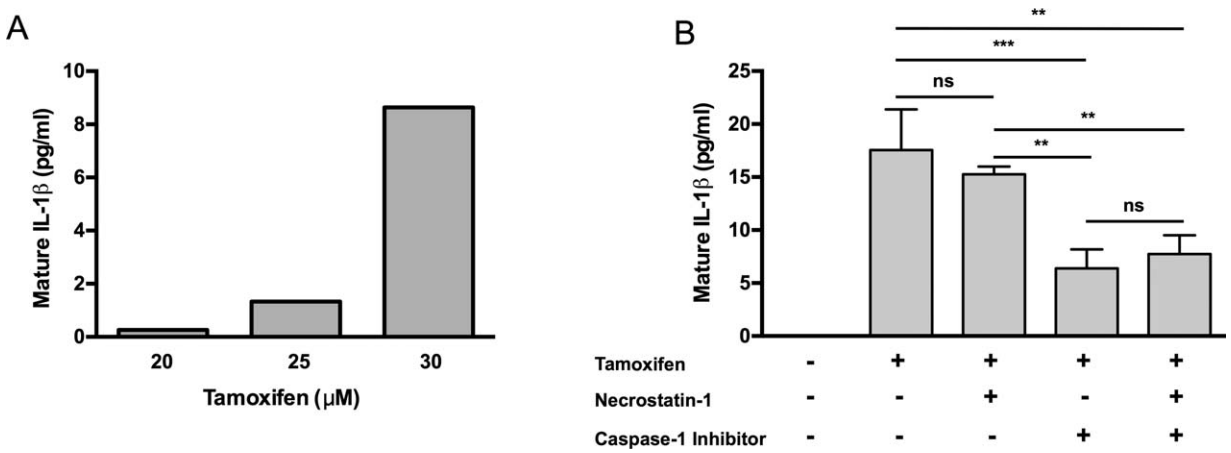


**Figure 6.** Tamoxifen toxicity results in IL-1β production in primed ARPE-19 cells. (**A**) IL-1β dose-response curve shows increasing levels of mature IL-1β production with increasing concentration of tamoxifen when primed with IL-1α. (**B**) ELISA for mature IL-1β shows that tamoxifen treatment of IL-1α–primed ARPE-19 cells results in mature IL-1β secretion. Inhibition of Nec-1 did not alter the levels of mature IL-1β secretion. Treatment with a caspase-1–specific inhibitor significantly decreased secretion of mature IL-1β; addition of Nec-1 did not affect IL-1β release. *Error bars*: ±SEM. Adjusted *P* values: $^{**}P < 0.05$, $^{***}P < 0.005$.

demonstrated to participate in pyroptosis, apoptosis, and necroptosis. Lysosomal destabilization and the associated release of hydrolases have been shown to activate the NLRP3 inflammasome in the RPE.[36] Inhibition of lysosomal cathepsins has been demonstrated to block NLRP3 signaling and caspase-1 activation in macrophages and lipopolysaccharide (LPS)-primed monocytes.[15,47,48] Moreover, cathepsins B and L have been found to mediate inflammasome activity in myeloid-derived cells.[49] Our observations that tamoxifen induces lysosomal destabilization prior to cell death and that inhibition of cathepsins B and L lead to almost complete blockage of tamoxifen-induced cytotoxicity are consistent with these previous reports.

In addition, cathepsins have been implicated in the process of apoptosis. Cytosolic cathepsins cleave the pro-apoptotic Bcl-2 family member BID, resulting in its activation, and degrade anti-apoptotic protein Bcl-2 proteins, triggering the intrinsic pathway of apoptosis.[50,51] Caspase-8 and -9 mediate the extrinsic and intrinsic pathways of apoptosis, respectively; and both of these initiator caspases can activate caspase-3. We demonstrate, as shown by others,[5] a significant role for the effector caspase-3 in tamoxifen cytotoxicity. Further, we have shown a primary role for the caspase-9–dependent intrinsic pathway, an observation that is indicative of mitochondrial dysfunction. This is in agreement with the finding that necroptosis can induce mitochondrial dysfunction, reactive oxygen species (ROS) formation,[23,26] and release of pro-apoptotic proteins of the Bcl-2 family.[52] Although the extrinsic pathway, which is caspase-8 dependent, does not seem to play a primary role in tamoxifen-mediated toxicity, others have reported that inhibition of caspase-8 activates RIP1 kinase.[53,54] Consistent with this finding, cotreatment with Nec-1 and a caspase-8 inhibitor led to near complete inhibition of cell death, greater than Nec-1 alone.

Cathepsins have also been shown to play a role in necroptosis, specifically, in caspase-compromised conditions; necroptosis can be arrested with application of cathepsin-B inhibitor CA-074-OMe.[55] Similarly, we have shown that combined cathepsin B and L inhibition leads to complete inhibition of cell death, and that cathepsin release occurs upstream of multiple cell death mechanisms. Necroptosis depends on the activity of the serine/threonine kinase RIP1, an adaptor kinase that functions downstream of death domain receptors and forms a complex with RIP3 to activate necroptosis. It is interesting to note that inhibition of RIP3 kinase activity will re-shuttle cell death toward apoptosis as catalytically inactive RIP3 kinase mutant engages RIP1, Fas-associated death domain (FADD), and caspase-8 complex and leads to caspase-8 activation, suggesting redundancy of cell death pathways.[56] Exposure of RPE cells to tamoxifen led to the activation of RIP1 and the initiation of necroptosis. As previously demonstrated in photoreceptors in a model of retinal detachment, cotreatment with caspase inhibitors and Nec-1 effectively suppresses photoreceptor cell death.[31,57,58] Accordingly, we found that suppression of tamoxifen cytotoxicity of the RPE requires concurrent treatment with caspase inhibitors and Nec-1.

Pathologic activation of the NLRP3 inflammasome and pyroptosis is characteristic of a variety of disease conditions in which lysosomal destabilization results from phagocytosis of crystals or insoluble aggregates.[16,17] For instance, silicosis and asbestosis are mediated by NLRP3 inflammasome activation in myeloid cells induced by silica crystals and asbestos fibers. Similarly, monosodium urate crystals cause gout via NLRP3 activation, and cholesterol crystals trigger NLRP3 during the development of atherosclerosis.[14] Previous work from our laboratory has demonstrated NLRP3 inflammasome expression in areas of geographic atrophy in the RPE of eyes from patients with AMD,[36] where we have hypothesized that it plays a role in its pathogenesis. Similarly, tamoxifen retinopathy is associated with the presence of retinal crystalline deposits and displays features similar to geographic atrophy with loss of the RPE and subsequent associated retinal atrophy.

The role of the NLRP3 inflammasome in tamoxifen toxicity of ARPE-19 cells is evidenced by the activation of caspase-1 with subsequent production of mature IL-1β and pyroptosis following tamoxifen treatment. Caspase-1 contributes to cell death through induction of pyroptosis; however, inhibition of caspase-1 significantly, but only partially, reduced cell death, indicating that while caspase-1 did contribute to tamoxifen-mediated RPE cell death, cell death was not mediated predominantly by pyroptosis alone. Thus, we suggest that multiple cell death mechanisms contribute to tamoxifen toxicity of the RPE.

A possible confounding factor is that tamoxifen competes with 7β-estradiol (E2) for binding to both nuclear receptors and plasma membrane estrogen receptors (ERs). Furthermore, ERs also are found in mitochondria, where E2 modulates

mitochondrial gene and protein expression,[59] and E2 is considered an anti-apoptotic agent, including prosurvival actions on human RPE challenged with oxidative stress.[60] In contrast, others have demonstrated ER-independent autophagic cell death by tamoxifen in breast cancer cells[61] and RPE cells.[5] In addition, E2-mediated cytoprotection of ARPE-19 cells was inhibited by ER antagonists ICI (ERα and ERβ) and THC (ERβ) but not by tamoxifen (ERα).[62] Our results are consistent with these previous findings that tamoxifen cytotoxicity occurs through an ER-independent mechanism of cell death.

Tamoxifen is a prodrug that is processed in the liver, yielding up to 40 different metabolites.[63] Analysis of human plasma using liquid-chromatography high-resolution mass spectrometry shows that a patient who received a very low dosage of tamoxifen for 5 years had 446 ng/mL or 1.2 μM of the parent drug. The potential CYP2D6 by-products α-OH-tamoxifen and 4-OH-tamoxifen represented only a small percentage of the prodrug (0.06% and 1.32%, respectively).[63] Thus, we have focused primarily on the tamoxifen prodrug, but we believe that the metabolic by-products of the parent drug, such as 4-OH-tamoxifen, can initiate cell death (Supplementary Fig. S1). We believe that both the tamoxifen prodrug and its metabolites can induce RPE death but that the degree of toxicity may vary in patients depending on dosage. Patients who take higher doses of tamoxifen may show relatively rapid signs of maculopathy, whereas patients who take low doses of the drug for a prolonged period of time show delayed signs of maculopathy owing to the accumulation of tamoxifen and its metabolites over time. The absolute quantification of the prodrug and all of its metabolites was thought to be unrealistic by Dahmane and colleagues.[63] We have shown that using relatively high concentrations of tamoxifen in vitro induces rapid RPE cell death, while lower concentrations of tamoxifen incite cell death over 2 weeks (Supplementary Fig. S2), demonstrating a cumulative insult to the RPE by tamoxifen.

Simultaneous inhibition of multiple cell death pathways may not be practical for therapeutic intervention. However, targeting factors upstream of all pathways involved would likely yield better outcomes with regard to safety and efficacy. As we have found that cathepsins B and L are key mediators of tamoxifen-induced RPE cytotoxicity, these proteases may be viable candidates for the development of pharmacologic inhibitors.

## *Acknowledgments*

The authors thank Magali Saint-Geniez, PhD (Schepens Eye Research Institute–Massachusetts Eye and Ear), for valuable discussion and advice and Christina Kaiser Marko, PhD, for editorial support.

Supported by National Eye Institute/National Institutes of Health (NEI/NIH) Grant K12-EY16335 and by the Massachusetts Lions Eye Research Fund (LAK); NIH Grants GM07226 and AG039245 (WAT); NEI Grant R21EY023079-01/A1, the Yeatts Family Foundation, a 2013 Macula Society Research Grant Award, and an Research to Prevent Blindness (RPB) Physician-Scientist Award (DGV); and NIH Grant EY015435 (PAD).

Disclosure: **L.A. Kim**, None; **D. Amarnani**, None; **G. Gnanaguru**, None; **W.A. Tseng**, None; **D.G. Vavvas**, P; **P.A. D'Amore**, None

## *References*

1. Davies C, Pan H, Godwin J, et al. Long-term effects of continuing adjuvant tamoxifen to 10 years versus stopping at 5 years after diagnosis of oestrogen receptor-positive breast cancer: ATLAS, a randomised trial. *Lancet*. 2013;381:805–816.
2. Nayfield SG, Gorin MB. Tamoxifen-associated eye disease: a review. *J Clin Oncol*. 1996;14:1018–1026.
3. Sadowski B, Kriegbaum C, Apfelstedt-Sylla E. Tamoxifen side effects, age-related macular degeneration (AMD) or cancer associated retinopathy (CAR)? *Eur J Ophthalmol*. 2001;11:309–312.
4. Chen PM, Gombart ZJ, Chen JW. Chloroquine treatment of ARPE-19 cells leads to lysosome dilation and intracellular lipid accumulation: possible implications of lysosomal dysfunction in macular degeneration. *Cell Biosci*. 2011;1:10.
5. Cho KS, Yoon YH, Choi JA, Lee SJ, Koh JY. Induction of autophagy and cell death by tamoxifen in cultured retinal pigment epithelial and photoreceptor cells. *Invest Ophthalmol Vis Sci*. 2012;53:5344–5353.
6. Nadim F, Walid H, Adib J. The differential diagnosis of crystals in the retina. *Int Ophthalmol*. 2001;24:113–121.
7. Heier JS, Dragoo RA, Enzenauer RW, Waterhouse WJ. Screening for ocular toxicity in asymptomatic patients treated with tamoxifen. *Am J Ophthalmol*. 1994;117:772–775.
8. Galluzzi L, Vitale I, Abrams JM, et al. Molecular definitions of cell death subroutines: recommendations of the Nomenclature Committee on Cell Death 2012. *Cell Death Differ*. 2012;19:107–120.
9. Bergsbaken T, Fink SL, Cookson BT. Pyroptosis: host cell death and inflammation. *Nat Rev Microbiol*. 2009;7:99–109.
10. Denes A, Lopez-Castejon G, Brough D. Caspase-1: is IL-1 just the tip of the ICEberg? *Cell Death Dis*. 2012;3:e338.
11. Feenstra DJ, Yego EC, Mohr S. Modes of retinal cell death in diabetic retinopathy. *J Clin Exp Ophthalmol*. 2013;4:298.
12. Dinarello CA. Interleukin-1 beta, interleukin-18, and the interleukin-1 beta converting enzyme. *Ann N Y Acad Sci*. 1998;856:1–11.
13. Fantuzzi G, Dinarello CA. Interleukin-18 and interleukin-1 beta: two cytokine substrates for ICE (caspase-1). *J Clin Immunol*. 1999;19:1–11.
14. Schroder K, Zhou R, Tschopp J. The NLRP3 inflammasome: a sensor for metabolic danger? *Science*. 2010;327:296–300.
15. Hornung V, Bauernfeind F, Halle A, et al. Silica crystals and aluminum salts activate the NALP3 inflammasome through phagosomal destabilization. *Nat Immunol*. 2008;9:847–856.
16. Halle A, Hornung V, Petzold GC, et al. The NALP3 inflammasome is involved in the innate immune response to amyloid-beta. *Nat Immunol*. 2008;9:857–865.
17. Dostert C, Petrilli V, Van Bruggen R, Steele C, Mossman BT, Tschopp J. Innate immune activation through Nalp3 inflammasome sensing of asbestos and silica. *Science*. 2008;320:674–677.
18. Jin C, Frayssinet P, Pelker R, et al. NLRP3 inflammasome plays a critical role in the pathogenesis of hydroxyapatite-associated arthropathy. *Proc Natl Acad Sci U S A*. 2011;108:14867–14872.
19. Cryns V, Yuan J. Proteases to die for. *Genes Dev*. 1998;12:1551–1570.
20. Robertson JD, Orrenius S. Role of mitochondria in toxic cell death. *Toxicology*. 2002;181–182:491–496.
21. Cheng AG, Cunningham LL, Rubel EW. Hair cell death in the avian basilar papilla: characterization of the in vitro model and caspase activation. *J Assoc Res Otolaryngol*. 2003;4:91–105.
22. Nicotera TM, Hu BH, Henderson D. The caspase pathway in noise-induced apoptosis of the chinchilla cochlea. *J Assoc Res Otolaryngol*. 2003;4:466–477.
23. Cho YS, Challa S, Moquin D, et al. Phosphorylation-driven assembly of the RIP1-RIP3 complex regulates programmed

necrosis and virus-induced inflammation. *Cell*. 2009;137: 1112–1123.

24. Cho Y, McQuade T, Zhang H, Zhang J, Chan FK. RIP1-dependent and independent effects of necrostatin-1 in necrosis and T cell activation. *PLoS One*. 2011;6:e23209.
25. Christofferson DE, Li Y, Hitomi J, et al. A novel role for RIP1 kinase in mediating TNFα production. *Cell Death Dis*. 2012;3: e320.
26. Zhang DW, Shao J, Lin J, et al. RIP3, an energy metabolism regulator that switches TNF-induced cell death from apoptosis to necrosis. *Science*. 2009;325:332–336.
27. Kono H, Rock KL. How dying cells alert the immune system to danger. *Nat Rev Immunol*. 2008;8:279–289.
28. Degterev A, Hitomi J, Germscheid M, et al. Identification of RIP1 kinase as a specific cellular target of necrostatins. *Nat Chem Biol*. 2008;4:313–321.
29. Hitomi J, Christofferson DE, Ng A, et al. Identification of a molecular signaling network that regulates a cellular necrotic cell death pathway. *Cell*. 2008;135:1311–1323.
30. Lu JV, Weist BM, van Raam BJ, et al. Complementary roles of Fas-associated death domain (FADD) and receptor interacting protein kinase-3 (RIPK3) in T-cell homeostasis and antiviral immunity. *Proc Natl Acad Sci U S A*. 2011;108:15312–15317.
31. Trichonas G, Murakami Y, Thanos A, et al. Receptor interacting protein kinases mediate retinal detachment-induced photoreceptor necrosis and compensate for inhibition of apoptosis. *Proc Natl Acad Sci U S A*. 2010;107:21695–21700.
32. Murakami Y, Matsumoto H, Roh M, et al. Programmed necrosis, not apoptosis, is a key mediator of cell loss and DAMP-mediated inflammation in dsRNA-induced retinal degeneration. *Cell Death Differ*. 2014;21:270–277.
33. Rosenbaum DM, Degterev A, David J, et al. Necroptosis, a novel form of caspase-independent cell death, contributes to neuronal damage in a retinal ischemia-reperfusion injury model. *J Neurosci Res*. 2010;88:1569–1576.
34. Stridh L, Smith PL, Naylor AS, Wang X, Mallard C. Regulation of toll-like receptor 1 and −2 in neonatal mice brains after hypoxia-ischemia. *J Neuroinflammation*. 2011;8:45.
35. Oerlemans MI, Liu J, Arslan F, et al. Inhibition of RIP1-dependent necrosis prevents adverse cardiac remodeling after myocardial ischemia-reperfusion in vivo. *Basic Res Cardiol*. 2012;107:270.
36. Tseng WA, Thein T, Kinnunen K, et al. NLRP3 inflammasome activation in retinal pigment epithelial cells by lysosomal destabilization: implications for age-related macular degeneration. *Invest Ophthalmol Vis Sci*. 2013;54:110–120.
37. Tarallo V, Hirano Y, Gelfand BD, et al. DICER1 loss and Alu RNA induce age-related macular degeneration via the NLRP3 inflammasome and MyD88. *Cell*. 2012;149:847–859.
38. Tschopp J, Schroder K. NLRP3 inflammasome activation: the convergence of multiple signalling pathways on ROS production? *Nat Rev Immunol*. 2010;10:210–215.
39. Ford KM, Saint-Geniez M, Walshe T, Zahr A, D'Amore PA. Expression and role of VEGF in the adult retinal pigment epithelium. *Invest Ophthalmol Vis Sci*. 2011;52:9478–9487.
40. Miao EA, Alpuche-Aranda CM, Dors M, et al. Cytoplasmic flagellin activates caspase-1 and secretion of interleukin 1beta via Ipaf. *Nat Immunol*. 2006;7:569–575.
41. Mannerstrom M, Zorn-Kruppa M, Diehl H, et al. Evaluation of the cytotoxicity of selected systemic and intravitreally dosed drugs in the cultures of human retinal pigment epithelial cell line and of pig primary retinal pigment epithelial cells. *Toxicol In Vitro*. 2002;16:193–200.
42. Wlodkowic D, Skommer J, Darzynkiewicz Z. Cytometry of apoptosis: historical perspective and new advances. *Exp Oncol*. 2012;34:255–262.
43. Lecoeur H, de Oliveira-Pinto LM, Gougeon ML. Multiparametric flow cytometric analysis of biochemical and functional events associated with apoptosis and oncosis using the 7-aminoactinomycin D assay. *J Immunol Methods*. 2002;265: 81–96.
44. Modest EJ, Sengupta SK. 7-Substituted actinomycin D (NSC-3053) analogs as fluorescent DNA-binding and experimental antitumor agents. *Cancer Chemother Rep*. 1974;58:35–48.
45. Lamkanfi M. Emerging inflammasome effector mechanisms. *Nat Rev Immunol*. 2011;11:213–220.
46. Ravanko K, Jarvinen K, Helin J, Kalkkinen N, Holtta E. Cysteine cathepsins are central contributors of invasion by cultured adenosylmethionine decarboxylase-transformed rodent fibroblasts. *Cancer Res*. 2004;64:8831–8838.
47. Hentze H, Lin XY, Choi MS, Porter AG. Critical role for cathepsin B in mediating caspase-1-dependent interleukin-18 maturation and caspase-1-independent necrosis triggered by the microbial toxin nigericin. *Cell Death Differ*. 2003;10:956–968.
48. Newman ZL, Leppla SH, Moayeri M. CA-074Me protection against anthrax lethal toxin. *Infect Immun*. 2009;77:4327–4336.
49. Keyel PA, Heid ME, Salter RD. Macrophage responses to bacterial toxins: a balance between activation and suppression. *Immunol Res*. 2011;50:118–123.
50. Turk B, Turk V. Lysosomes as "suicide bags" in cell death: myth or reality? *J Biol Chem*. 2009;284:21783–21787.
51. Droga-Mazovec G, Bojic L, Petelin A, et al. Cysteine cathepsins trigger caspase-dependent cell death through cleavage of bid and antiapoptotic Bcl-2 homologues. *J Biol Chem*. 2008;283: 19140–19150.
52. Kroemer G, Galluzzi L, Brenner C. Mitochondrial membrane permeabilization in cell death. *Physiol Rev*. 2007;87:99–163.
53. Yu L, Alva A, Su H, et al. Regulation of an ATG7-beclin 1 program of autophagic cell death by caspase-8. *Science*. 2004; 304:1500–1502.
54. He S, Wang L, Miao L, et al. Receptor interacting protein kinase-3 determines cellular necrotic response to TNF-alpha. *Cell*. 2009;137:1100–1111.
55. Dunai ZA, Imre G, Barna G, et al. Staurosporine induces necroptotic cell death under caspase-compromised conditions in U937 cells. *PLoS One*. 2012;7:e41945.
56. Newton K, Dugger DL, Wickliffe KE, et al. Activity of protein kinase RIPK3 determines whether cells die by necroptosis or apoptosis. *Science*. 2014;343:1357–1360.
57. Murakami Y, Miller JW, Vavvas DG. RIP kinase-mediated necrosis as an alternative mechanisms of photoreceptor death. *Oncotarget*. 2011;2:497–509.
58. Murakami Y, Matsumoto H, Roh M, et al. Receptor interacting protein kinase mediates necrotic cone but not rod cell death in a mouse model of inherited degeneration. *Proc Natl Acad Sci U S A*. 2012;109:14598–14603.
59. Chen JQ, Cammarata PR, Baines CP, Yager JD. Regulation of mitochondrial respiratory chain biogenesis by estrogens/estrogen receptors and physiological, pathological and pharmacological implications. *Biochim Biophys Acta*. 2009;1793: 1540–1570.
60. Marin-Castano ME, Striker GE, Alcazar O, Catanuto P, Espinosa-Heidmann DG, Cousins SW. Repetitive nonlethal oxidant injury to retinal pigment epithelium decreased extracellular

Investigative Ophthalmology & Visual Science

matrix turnover in vitro and induced sub-RPE deposits in vivo. *Invest Ophthalmol Vis Sci*. 2006;47:4098–4112.

61. Hwang JJ, Kim HN, Kim J, et al. Zinc(II) ion mediates tamoxifen-induced autophagy and cell death in MCF-7 breast cancer cell line. *Biometals*. 2010;23:997–1013.
62. Giddabasappa A, Bauler M, Yepuru M, Chaum E, Dalton JT, Eswaraka J. 17-beta estradiol protects ARPE-19 cells from oxidative stress through estrogen receptor-beta. *Invest Ophthalmol Vis Sci*. 2010;51:5278–5287.
63. Dahmane E, Boccard J, Csajka C, et al. Quantitative monitoring of tamoxifen in human plasma extended to 40 metabolites using liquid-chromatography high-resolution mass spectrometry: new investigation capabilities for clinical pharmacology. *Anal Bioanal Chem*. 2014;406:2627–2640.

Investigative Ophthalmology & Visual Science